Figure S1

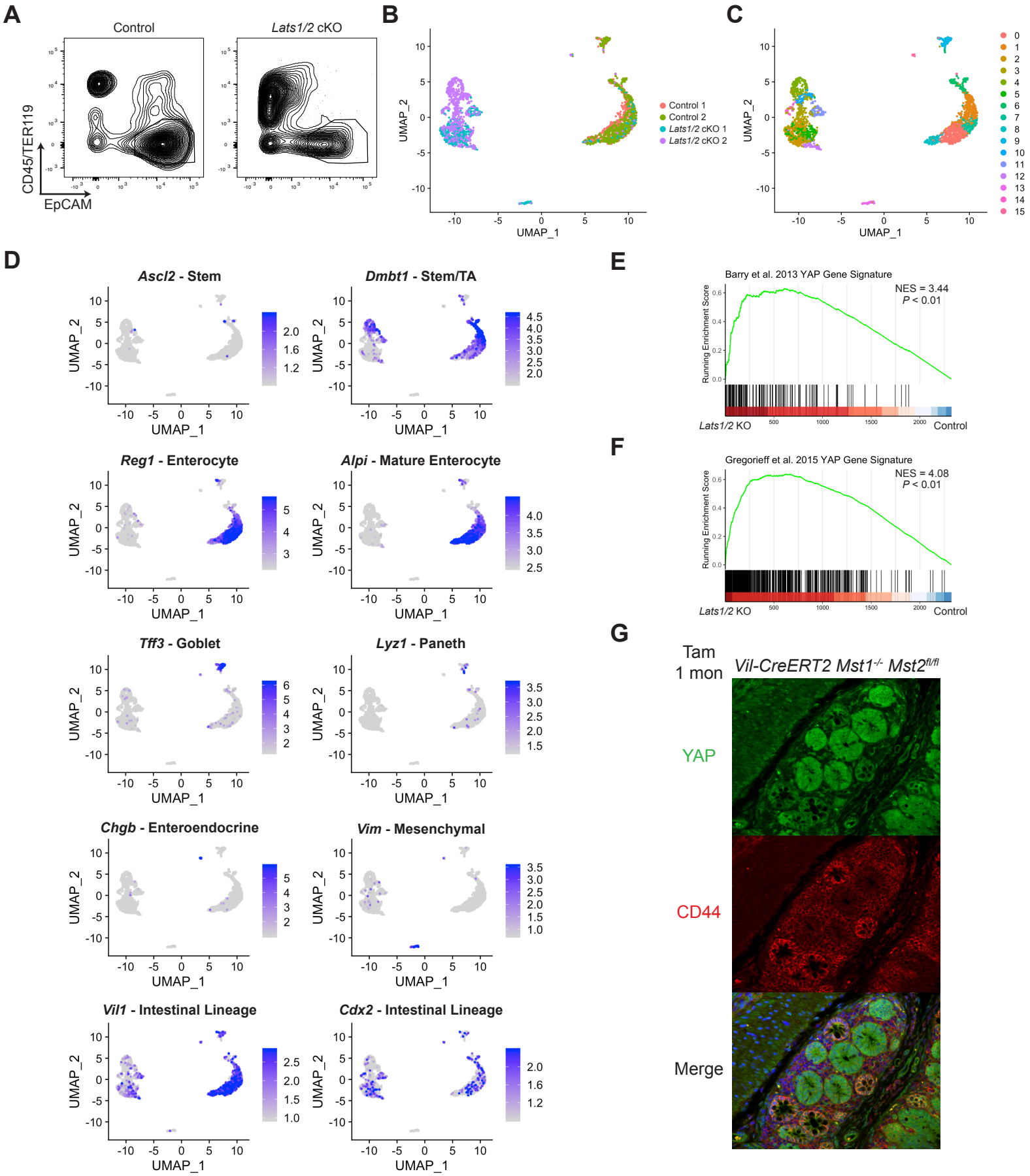
A
Control
Lats1/2 cKO
CD45/TER119
EpCAM
B
UMAP_2
UMAP_1
Control 1
Control 2
Lats1/2 cKO 1
Lats1/2 cKO 2
C
UMAP_2
UMAP_1
0
1
2
3
4
5
6
7
8
9
10
11
12
13
14
15
D
Ascl2 - Stem
Dmbt1 - Stem/TA
Reg1 - Enterocyte
Alpi - Mature Enterocyte
Tff3 - Goblet
Lyz1 - Paneth
Chgb - Enteroendocrine
Vim - Mesenchymal
Vil1 - Intestinal Lineage
Cdx2 - Intestinal Lineage
UMAP_2
UMAP_1
E
Barry et al. 2013 YAP Gene Signature
NES = 3.44
P < 0.01
Running Enrichment Score
Lats1/2 KO
Control
F
Gregorieff et al. 2015 YAP Gene Signature
NES = 4.08
P < 0.01
Running Enrichment Score
Lats1/2 KO
Control
G
Tam
1 mon
Vil-CreERT2 Mst1-/- Mst2fl/fl
YAP
CD44
Merge

Figure S1: Single Cell Analysis of Intestinal *Lats1/2* Knockout Cells, Related to Figure 1

(A) Gating strategy for isolation of intestinal epithelial cells by FACS. Cells from control and *Lats1/2* cKO mice were sorted on forward scatter and side scatter and subsequently by EpCAM+, Lin- (CD45, TER119), and DAPI-. Sorted cells were encapsulated for scRNA-seq.

(B) UMAP representation of scRNA-seq data of intestinal epithelial cells from 2 control and 2 *Lats1/2* cKO animals in the indicated colors.

(C) Unsupervised clustering of control and *Lats1/2* cKO cells.

(D) UMAP showing normalized expression of cell-type specific markers.

(E-F) GSEA of a YAP gene signature from Barry et al., 2013 (E) and Gregorieff et al., 2015 (F) in *Lats1/2* KO cells compared to control cells.

(G) IF for YAP (green) and CD44 (red) in crypts of *Vil-CreERT2 Mst1*$^{-/-}$ *Mst2*$^{fl/fl}$ mice 1 month after tamoxifen injection. Sections were counterstained with DAPI (blue).

Figure S2

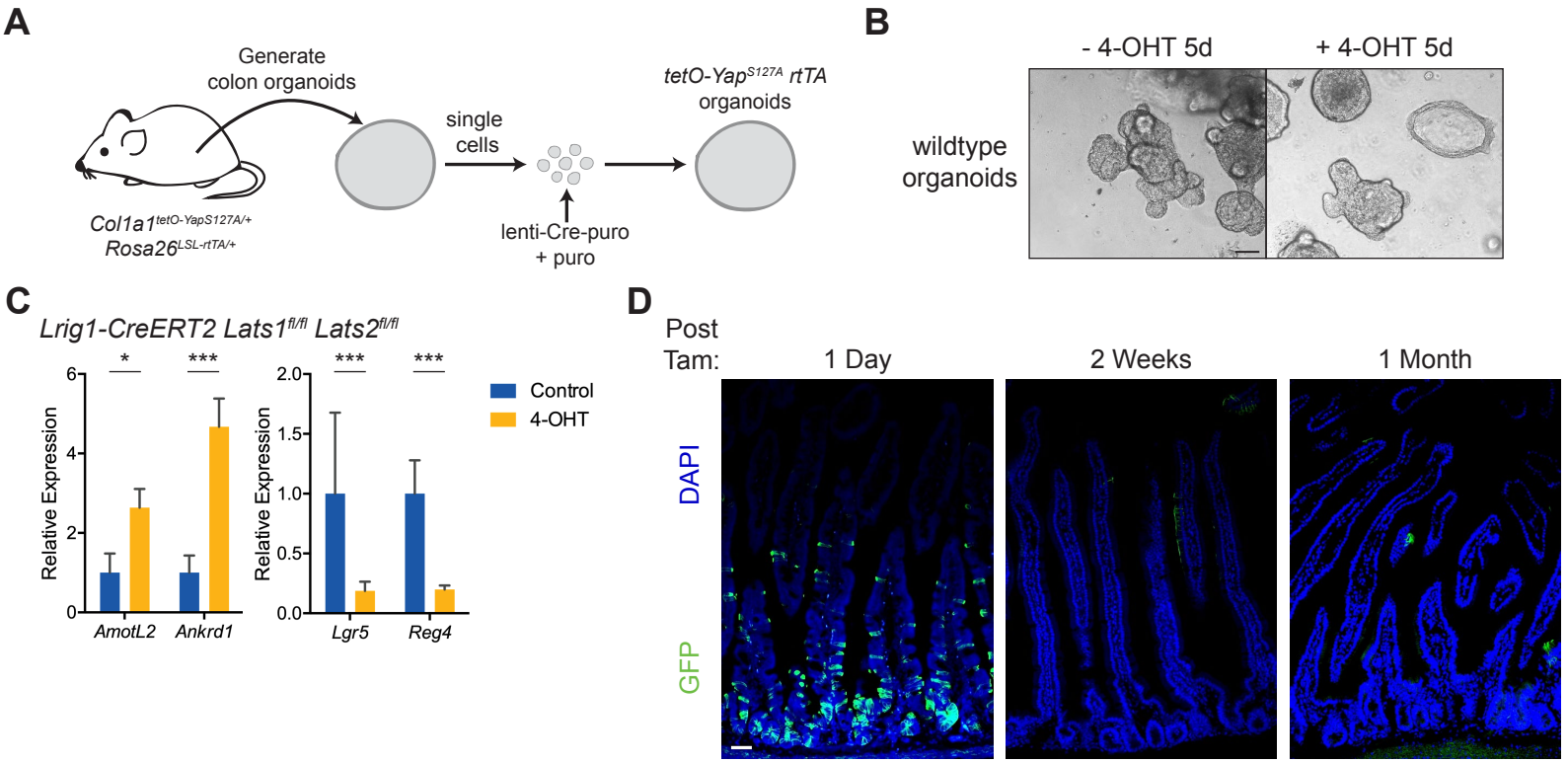

Figure S2: YAP Suppresses Stem Cell Function, Related to Figure 2

(A) Schematic for generating *tetO-YAP^{S127A} rtTA* organoids.

(B) Brightfield images of wildtype colon organoids five days after treatment with 4-OHT for 24 hours. Scale bar, 200 μm.

(C) RT-qPCR analysis of the indicated genes in *Lrig1-CreERT2 Lats1$^{fl/fl}$ Lats2$^{fl/fl}$* organoids 2 days after induction with 4-OHT for 24 hours. Data are represented as mean ± SEM; n = 2 biological and 2 technical replicates. **P* < 0.05 and ****P* < 0.001.

(D) IF for GFP and DAPI in the small intestine of *Lgr5-CreERT2 Lats1$^{fl/fl}$ Lats2$^{fl/fl}$ Rosa26$^{mT/mG}$* at the indicated times after the second injection with tamoxifen.

Figure S3

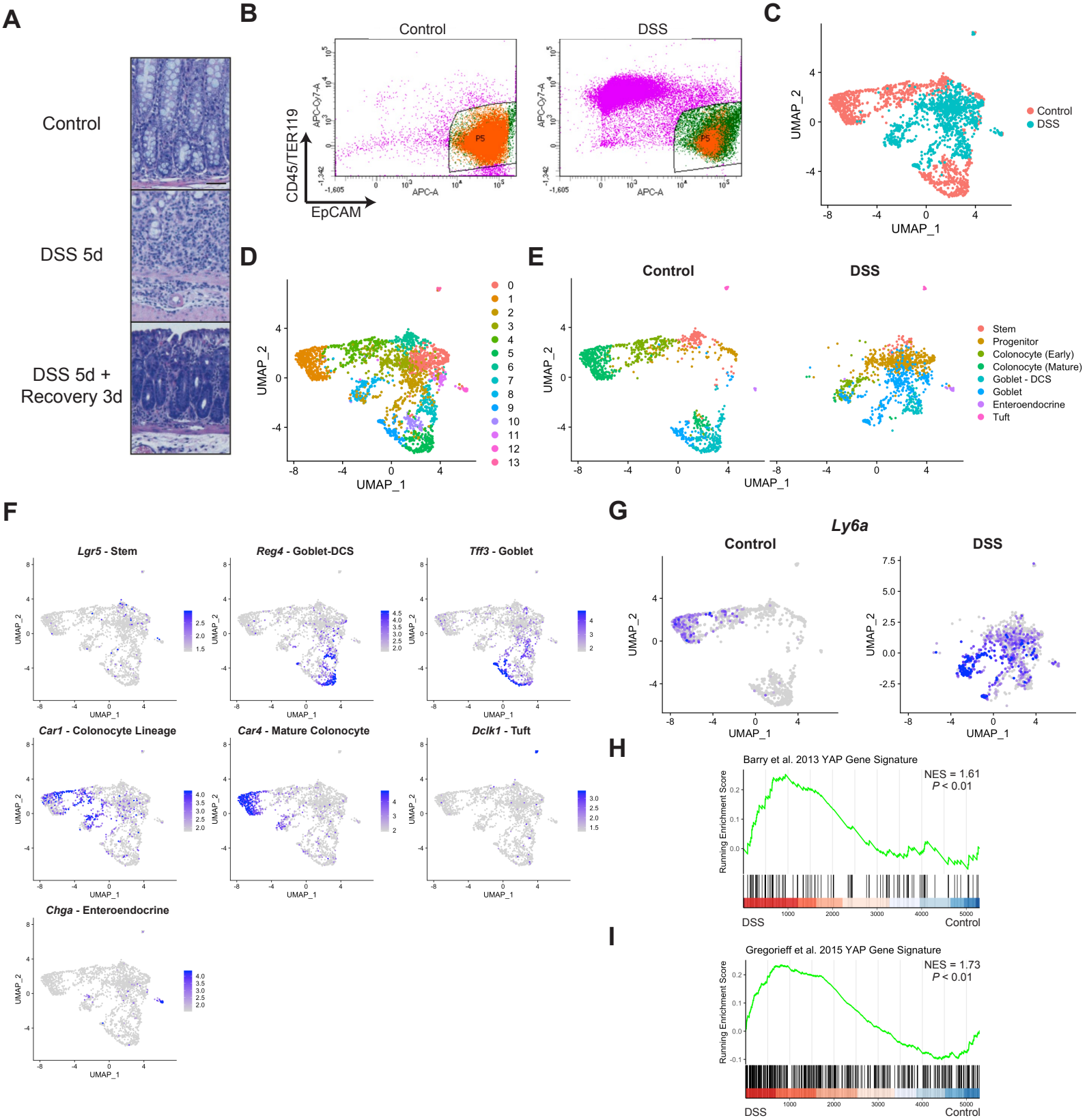
A
Control
DSS 5d
DSS 5d +
Recovery 3d
B
Control
DSS
CD45/TER119
EpCAM
APC-Cy7-A
APC-A
P5
C
UMAP_2
UMAP_1
Control
DSS
D
UMAP_2
UMAP_1
0
1
2
3
4
5
6
7
8
9
10
11
12
13
E
Control
DSS
UMAP_2
UMAP_1
Stem
Progenitor
Colonocyte (Early)
Colonocyte (Mature)
Goblet - DCS
Goblet
Enteroendocrine
Tuft
F
Lgr5 - Stem
Reg4 - Goblet-DCS
Tff3 - Goblet
Car1 - Colonocyte Lineage
Car4 - Mature Colonocyte
Dclk1 - Tuft
Chga - Enteroendocrine
UMAP_2
UMAP_1
G
Ly6a
Control
DSS
UMAP_2
UMAP_1
H
Barry et al. 2013 YAP Gene Signature
NES = 1.61
P < 0.01
Running Enrichment Score
DSS
Control
I
Gregorieff et al. 2015 YAP Gene Signature
NES = 1.73
P < 0.01
Running Enrichment Score
DSS
Control

Figure S3: Single Cell Analysis of Regenerating Epithelial Cells, Related to Figure 3

(A) H&E stains of colonic samples from mice following DSS treatment with or without recovery. Scale bar, 50 μm.

(B) Gating strategy for isolation of colonic epithelial cells by FACS. Cells from control and DSS-treated mice, following a 3-day recovery period, were sorted on forward scatter and side scatter and subsequently by EpCAM+, Lin- (CD45, TER119), and DAPI-. Sorted cells were encapsulated for scRNA-seq.

(C) UMAP representation of scRNA-seq data of colonic epithelial cells from control and DSS-treated mice, following a 3-day recovery period, in the indicated colors.

(D) Unsupervised clustering of the DSS and control samples.

(E) UMAP showing cell types in the indicated colors by treatment group.

(F) UMAP showing normalized expression of cell-type specific markers.

(G) UMAP showing normalized expression of *Ly6a/Sca1* in control and DSS samples.

(H-I) GSEA of a YAP gene signature from Barry et al., 2013 (H) and Gregorieff et al., 2015 (I) in DSS compared to control.

Figure S4

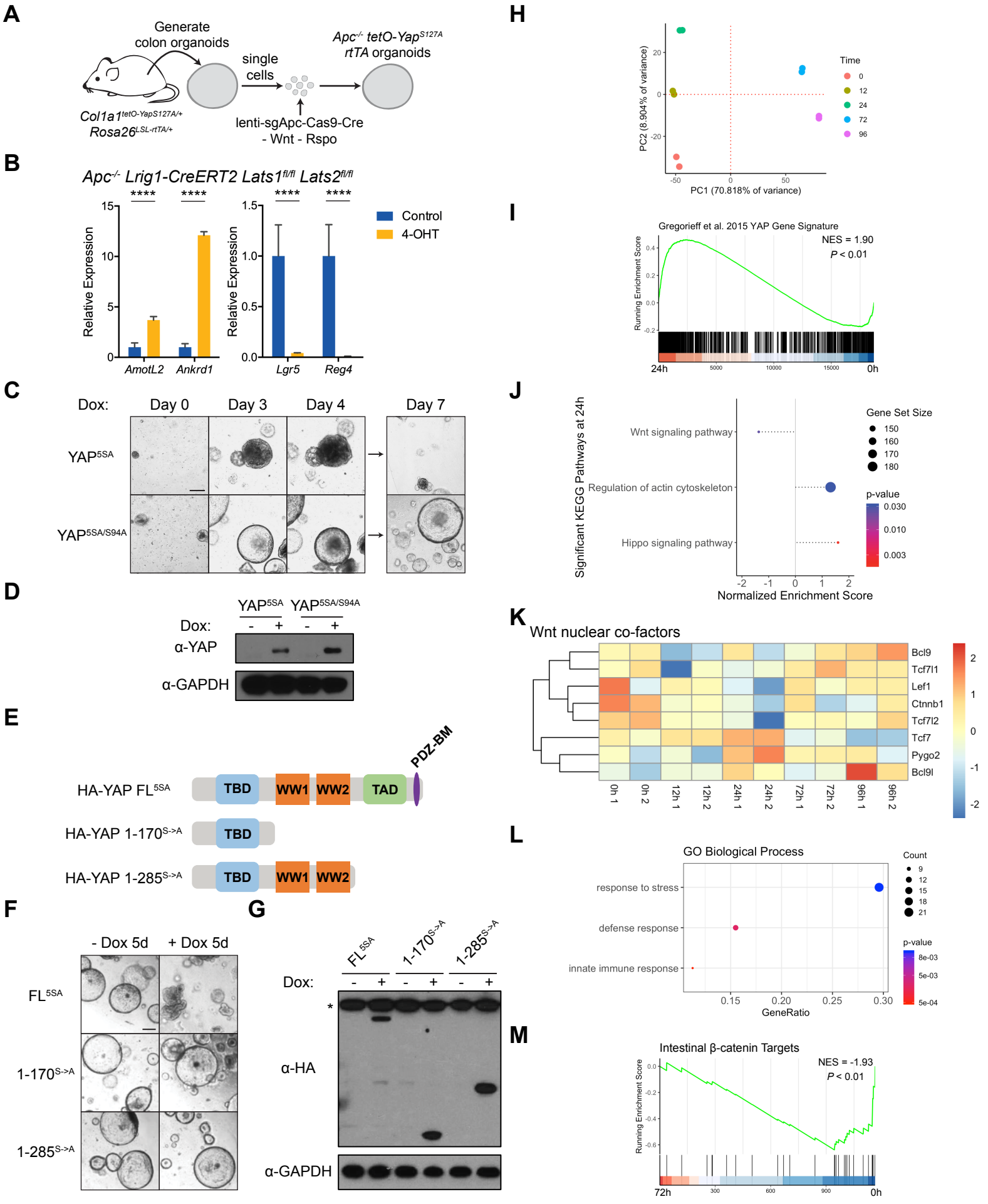
A
Generate colon organoids
single cells
Apc-/- tetO-Yap S127A rtTA organoids
Col1a1 tetO-YapS127A/+ Rosa26 LSL-rtTA/+
lenti-sgApc-Cas9-Cre - Wnt - Rspo
B
Apc-/- Lrig1-CreERT2 Lats1 fl/fl Lats2 fl/fl
Relative Expression
AmotL2
Ankrd1
Lgr5
Reg4
Control
4-OHT
C
Dox:
Day 0
Day 3
Day 4
Day 7
YAP5SA
YAP5SA/S94A
D
YAP5SA
YAP5SA/S94A
Dox:
α-YAP
α-GAPDH
E
PDZ-BM
HA-YAP FL5SA
HA-YAP 1-170S->A
HA-YAP 1-285S->A
TBD
WW1
WW2
TAD
F
- Dox 5d
+ Dox 5d
FL5SA
1-170S->A
1-285S->A
G
FL5SA
1-170S->A
1-285S->A
Dox:
α-HA
α-GAPDH
H
PC2 (8.904% of variance)
PC1 (70.818% of variance)
Time
I
Gregorieff et al. 2015 YAP Gene Signature
NES = 1.90
P < 0.01
Running Enrichment Score
24h
0h
J
Significant KEGG Pathways at 24h
Wnt signaling pathway
Regulation of actin cytoskeleton
Hippo signaling pathway
Normalized Enrichment Score
Gene Set Size
p-value
K
Wnt nuclear co-factors
Bcl9
Tcf7l1
Lef1
Ctnnb1
Tcf7l2
Tcf7
Pygo2
Bcl9l
0h 1
0h 2
12h 1
12h 2
24h 1
24h 2
72h 1
72h 2
96h 1
96h 2
L
GO Biological Process
response to stress
defense response
innate immune response
GeneRatio
Count
p-value
M
Intestinal β-catenin Targets
NES = -1.93
P < 0.01
Running Enrichment Score
72h
0h

Figure S4: YAP Mediates Transcriptional Reprogramming of *Apc*$^{-/-}$ Colon Cells, Related to Figure 4

(A) Schematic for generating *Apc*$^{-/-}$ *tetO-YAP*^{S127A} *rtTA* organoids.

(B) RT-qPCR analysis of the indicated genes in *Apc*$^{-/-}$ *Lrig1-CreERT2 Lats1/2*$^{fl/fl}$ organoids 2 days after induction with 4-OHT for 24 hours. Data are represented as mean ± SEM; n = 2 biological and 2 technical replicates. ****$P < 0.0001$.

(C) Brightfield images of *Apc*$^{-/-}$ *CAGs-rtTA3* organoids expressing doxycycline-inducible Yap^{5SA} or YAP$^{5SA/S94A}$ on the indicated days in the presence of doxycycline. The organoids were split on day 4. Scale bar, 200 μm.

(D) Western blot analysis of *Apc*$^{-/-}$ *CAGs-rtTA3* organoids expressing inducible YAP^{5SA} or YAP$^{5SA/S94A}$ after 2 days on doxycycline. Antibodies are indicated.

(E) Schematic of the domain architecture of HA-tagged Yap^{5SA}: full-length (FL), amino acids 1-170, and amino acids 1-285.

(F) Brightfield images of *Apc*$^{-/-}$ *CAGs-rtTA3* organoids expressing inducible deletion versions of HA-tagged Yap^{5SA} for 5 days. Scale bar, 200 μm.

(G) Western blot analysis of *Apc*$^{-/-}$ *CAGs-rtTA3* organoids expressing inducible deletion versions of HA-tagged YAP^{5SA} after 2 days on doxycycline. Antibodies are indicated. The asterisk indicates a non-specific band.

(H) Principal component analysis of whole transcriptome profiles of *Apc*$^{-/-}$ *tetO-YAP*^{S127A} *rtTA* organoids at the indicated hours following doxycycline induction.

(I-J) GSEA of a YAP gene signature from Gregorieff et al., 2015 (I) and KEGG pathways (J) in *Apc*$^{-/-}$ *tetO-YAP*^{S127A} *rtTA* organoids 24 hours after doxycycline compared to 0 hours.

(K) Heatmap of Wnt signaling pathway nuclear co-factors over the time course of doxycycline induction in *Apc*$^{-/-}$ *tetO-YAP*^{S127A} *rtTA* organoids.

(L) GO overrepresentation analysis of upregulated transcription factors (adjusted p-value < 0.05 and $\log_2$ fold change > 1) in *Apc*$^{-/-}$ *tetO-YAP*^{S127A} *rtTA* organoids after 72 hours on doxycycline compared to 0 hours.

(M) GSEA of intestinal β-catenin targets in differentially expressed transcription factors in *Apc*$^{-/-}$ *tetO-YAP*^{S127A} *rtTA* organoids after 72 hours on doxycycline compared to 0 hours.

Figure S5

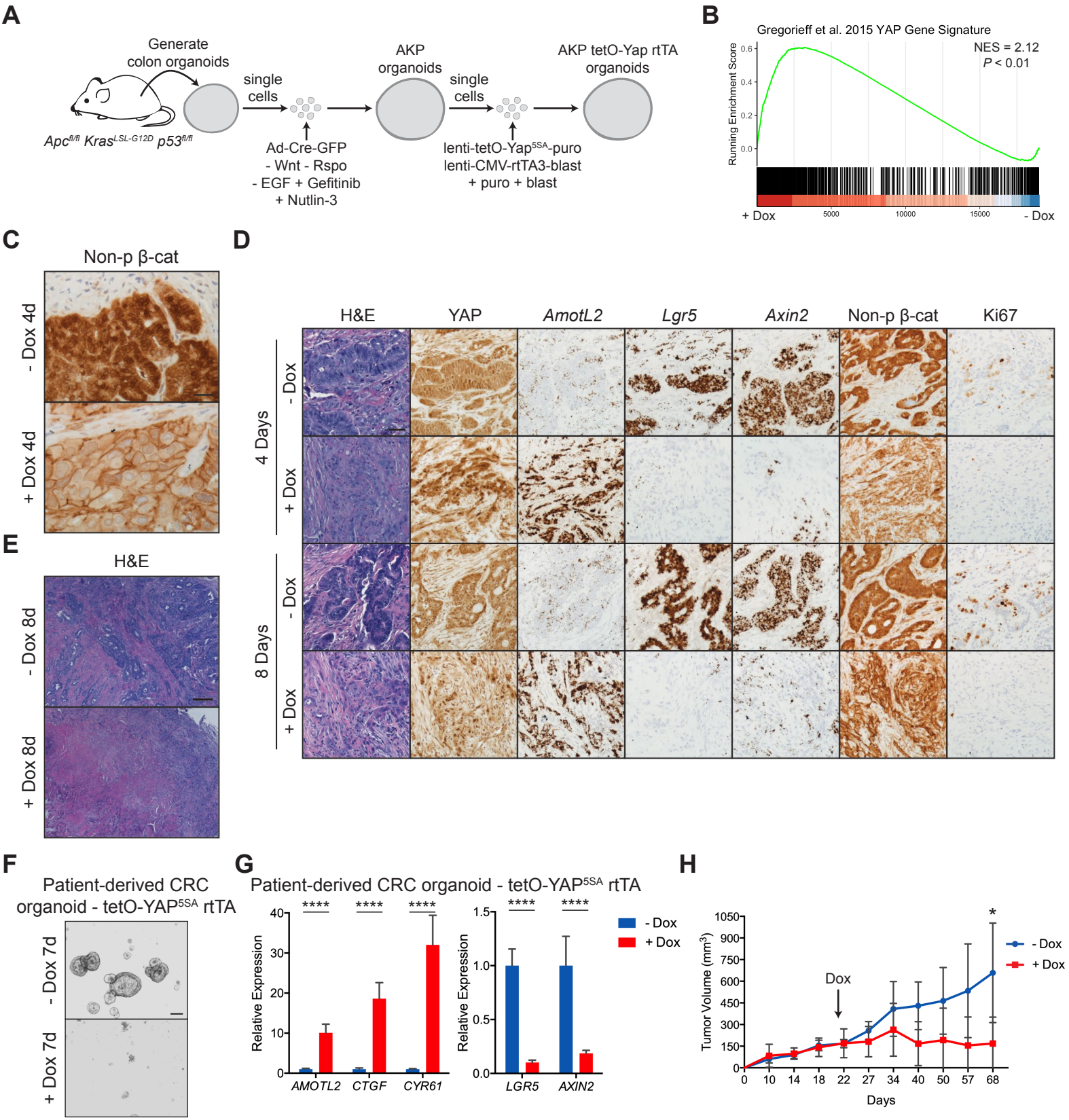
A
Generate colon organoids
Apc^fl/fl Kras^LSL-G12D p53^fl/fl
single cells
Ad-Cre-GFP - Wnt - Rspo - EGF + Gefitinib + Nutlin-3
AKP organoids
single cells
lenti-tetO-Yap5SA-puro lenti-CMV-rtTA3-blast + puro + blast
AKP tetO-Yap rtTA organoids
B
Gregorieff et al. 2015 YAP Gene Signature
NES = 2.12
P < 0.01
Running Enrichment Score
+ Dox
- Dox
C
Non-p β-cat
- Dox 4d
+ Dox 4d
D
H&E
YAP
AmotL2
Lgr5
Axin2
Non-p β-cat
Ki67
4 Days
8 Days
- Dox
+ Dox
E
H&E
- Dox 8d
+ Dox 8d
F
Patient-derived CRC organoid - tetO-YAP5SA rtTA
- Dox 7d
+ Dox 7d
G
Patient-derived CRC organoid - tetO-YAP5SA rtTA
Relative Expression
AMOTL2
CTGF
CYR61
LGR5
AXIN2
- Dox
+ Dox
H
Tumor Volume (mm3)
Dox
Days
- Dox
+ Dox

Figure S5: YAP Activation Causes Colon Tumor Regression, Related to Figure 5

(A) Schematic for generating *Apc*$^{-/-}$ *Kras*^{G12D} *p53*$^{-/-}$ tetO-YAP^{5SA} rtTA organoids.

(B) GSEA of a YAP gene signature from Gregorieff et al., 2015 in *Apc*$^{-/-}$ *Kras*^{G12D} *p53*$^{-/-}$ tetO-YAP^{5SA} rtTA organoids 3 days after induction with doxycycline.

(C) IHC for non-phosphorylated β-catenin from *Apc*$^{-/-}$ *Kras*^{G12D} *p53*$^{-/-}$ rtTA tetO-YAP^{5SA} orthotopic tumors 4 days after doxycycline administration. Scale bar, 50 μm.

(D) Histological analysis of *Apc*$^{-/-}$ *Kras*^{G12D} *p53*$^{-/-}$ tetO-YAP^{5SA} rtTA subcutaneous tumors on the indicated days following doxycycline administration: H&E stains, IHC for YAP, non-phosphorylated β-catenin, and Ki67, and RNA-ISH for *AmotL2, Lgr5*, and *Axin2*. Scale bar, 50 μm.

(E) H&E stains of *Apc*$^{-/-}$ *Kras*^{G12D} *p53*$^{-/-}$ tetO-YAP^{5SA} rtTA subcutaneous tumors 8 days after doxycycline administration. Scale bar, 200 μm.

(F) Brightfield images of a patient-derived CRC organoid line with inducible YAP^{5SA} overexpression after 7 days in the presence or absence of doxycycline. The organoids were split on day 4. Scale bar, 200 μm.

(G) RT-qPCR analysis of the indicated genes in patient-derived CRC organoids overexpressing YAP^{5SA}. Data are represented as mean ± SEM; n = 2 biological and 2 technical replicates. ****$P < 0.0001$.

(H) Growth curve of subcutaneous tumors from patient-derived CRC organoids overexpressing YAP^{5SA} injected in the flanks of nude mice. The arrow indicates the day doxycycline treatment was started. Measurements were started one week after injection (shown as day 0 on the graph). Data are represented as mean ± SD. *$P < 0.05$.

Figure S6

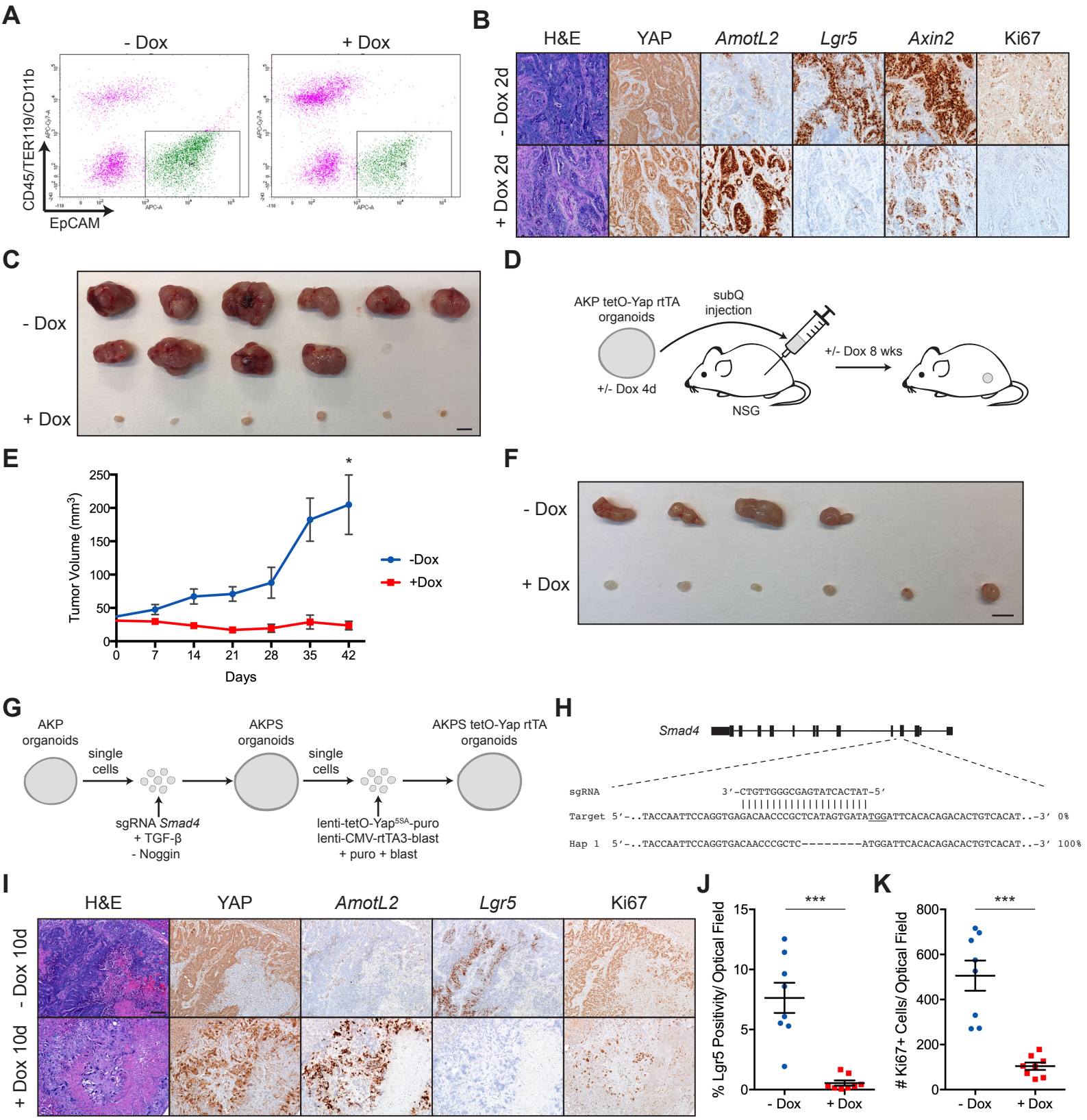
A
- Dox
+ Dox
CD45/TER119/CD11b
EpCAM
B
H&E
YAP
AmotL2
Lgr5
Axin2
Ki67
- Dox 2d
+ Dox 2d
C
- Dox
+ Dox
D
AKP tetO-Yap rtTA organoids
subQ injection
+/- Dox 4d
NSG
+/- Dox 8 wks
E
Tumor Volume (mm3)
Days
-Dox
+Dox
F
- Dox
+ Dox
G
AKP organoids
single cells
sgRNA Smad4
+ TGF-β
- Noggin
AKPS organoids
single cells
lenti-tetO-Yap5SA-puro
lenti-CMV-rtTA3-blast
+ puro + blast
AKPS tetO-Yap rtTA organoids
H
Smad4
sgRNA 3'-CTGTTGGGCGAGTATCACTAT-5'
Target 5'-..TACCAATTCCAGGTGAGACAACCCGCTCATAGTGATATGGATTCACACAGACACTGTCACAT..-3' 0%
Hap 1 5'-..TACCAATTCCAGGTGACAACCCGCTC---------ATGGATTCACACAGACACTGTCACAT..-3' 100%
I
H&E
YAP
AmotL2
Lgr5
Ki67
- Dox 10d
+ Dox 10d
J
% Lgr5 Positivity/ Optical Field
***
- Dox
+ Dox
K
Ki67+ Cells/ Optical Field
***
- Dox
+ Dox

Figure S6: YAP Suppresses Tumor Propagating Capacity in Primary and Metastatic CRC, Related to Figure 6

(A) Gating strategy for isolation of *Apc*$^{-/-}$ *Kras*^{G12D} *p53*$^{-/-}$ tetO-YAP^{5SA} rtTA subcutaneous primary tumor cells by FACS. Tumor cells from induced and uninduced mice were sorted on forward scatter and side scatter and subsequently by EpCAM+, Lin- (CD45, TER119, CD11b), and DAPI-. Sorted cells were then injected subcutaneously into nude mice for secondary transplants.

(B) Histological analysis of *Apc*$^{-/-}$ *Kras*^{G12D} *p53*$^{-/-}$ tetO-YAP^{5SA} rtTA subcutaneous primary tumors 2 days after doxycycline administration: H&E stains, IHC for YAP and Ki67, and RNA-ISH for *AmotL2*, *Lgr5,* and *Axin2*. Scale bar, 50 μm.

(C) Gross morphology of *Apc*$^{-/-}$ *Kras*^{G12D} *p53*$^{-/-}$ tetO-YAP^{5SA} rtTA subcutaneous tumors harvested 5 weeks following secondary transplant. Scale bar, 5 mm.

(D) Schematic of subcutaneous transplants of doxycycline-induced *Apc*$^{-/-}$ *Kras*^{G12D} *p53*$^{-/-}$ tetO-YAP^{5SA} rtTA organoids into nude mice and doxycycline administration.

(E) Growth curve of subcutaneous tumors from uninduced and doxycycline-induced *Apc*$^{-/-}$ *Kras*^{G12D} *p53*$^{-/-}$ tetO-YAP^{5SA} rtTA organoids injected into the flanks of nude mice. Measurements were started one week after injection (shown as day 0 on the graph). Data are represented as mean ± SEM; - dox: n = 6 tumors; + dox: n = 4 tumors. **P* < 0.05.

(F) Gross morphology of subcutaneous tumors derived from uninduced or induced *Apc*$^{-/-}$ *Kras*^{G12D} *p53*$^{-/-}$ tetO-YAP^{5SA} rtTA organoids 8 weeks following transplant. Scale bar, 5 mm.

(G) Schematic for generating *Apc*$^{-/-}$ *Kras*^{G12D} *p53*$^{-/-}$ *Smad4*$^{-/-}$ tetO-YAP^{5SA} rtTA organoids.

(H) Gene-targeting strategy for *Smad4*. The protospacer adjacent motif is underlined on the target sequence, and the allelic fraction of the haplotype identified is indicated.

(I) Histological analysis of *Apc*$^{-/-}$ *Kras*^{G12D} *p53*$^{-/-}$ *Smad4*$^{-/-}$ tetO-YAP^{5SA} rtTA metastases 10 days after doxycycline administration: H&E stains, IHC for YAP and Ki67, and RNA-ISH for *AmotL2* and *Lgr5*. Scale bar, 100 μm.

(J) Quantification of *Lgr5* positive staining in uninduced and induced *Apc*$^{-/-}$ *Kras*^{G12D} *p53*$^{-/-}$ *Smad4*$^{-/-}$ tetO-YAP^{5SA} rtTA metastases from Figure S6I. Dot plot is represented as mean ± SEM; - dox: n = 4 optical fields per mouse, n = 2 mice; + dox: n = 2 optical fields per mouse, n = 4 mice. ****P* < 0.001.

(K) Quantification of Ki67+ cells per high powered optical field in uninduced and induced *Apc*$^{-/-}$ *Kras*^{G12D} *p53*$^{-/-}$ *Smad4*$^{-/-}$ tetO-YAP^{5SA} rtTA metastases from Figure S6I. Dot plot is represented as mean ± SEM; - dox: n = 4 optical fields per mouse, n = 2 mice; + dox: n = 2 optical fields per mouse, n = 4 mice. ****P* < 0.001.

Figure S7

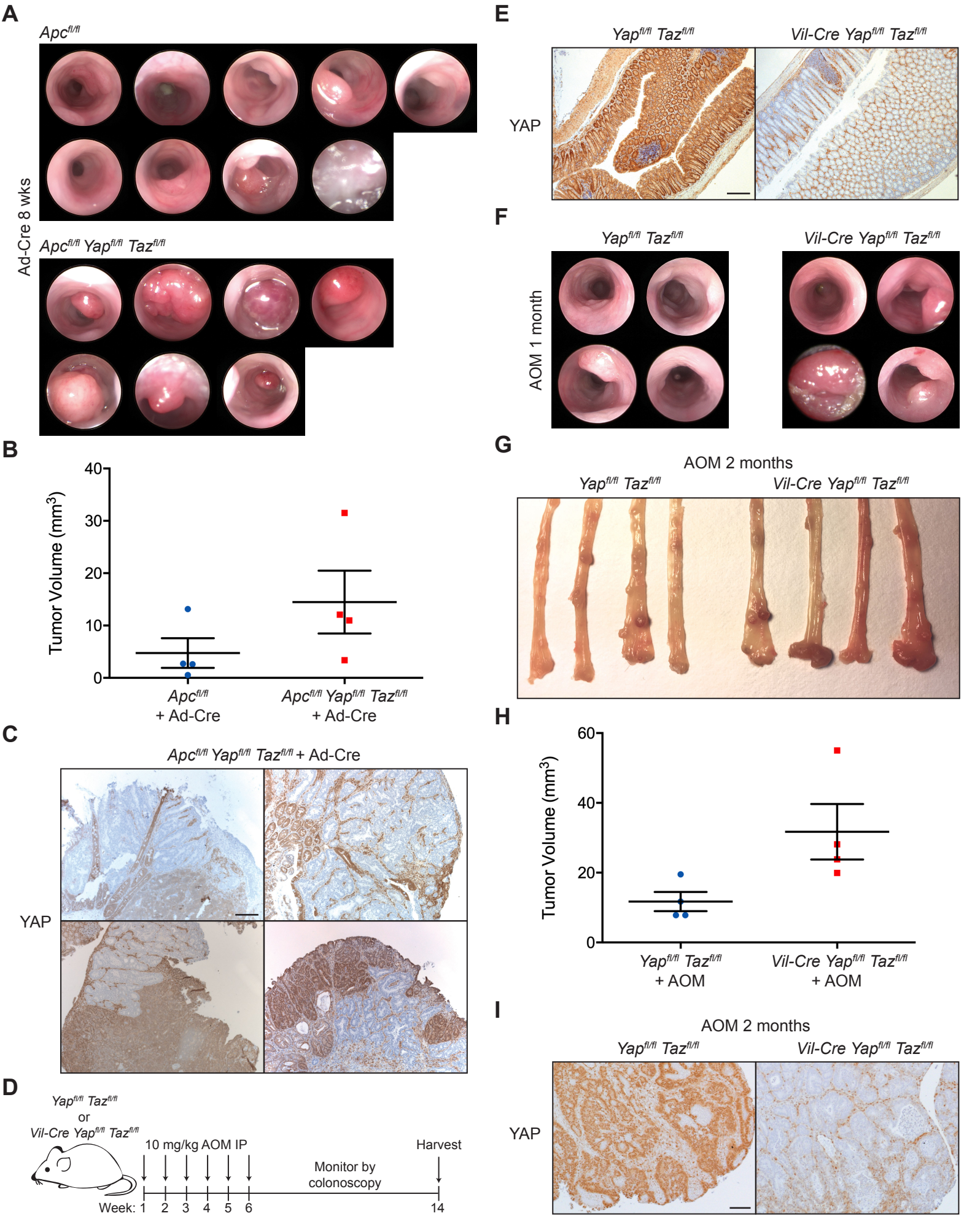
A
Apc fl/fl
Ad-Cre 8 wks
Apc fl/fl Yap fl/fl Taz fl/fl
B
Tumor Volume (mm3)
40
30
20
10
0
Apc fl/fl + Ad-Cre
Apc fl/fl Yap fl/fl Taz fl/fl + Ad-Cre
C
Apc fl/fl Yap fl/fl Taz fl/fl + Ad-Cre
YAP
D
Yap fl/fl Taz fl/fl
or
Vil-Cre Yap fl/fl Taz fl/fl
10 mg/kg AOM IP
Harvest
Monitor by colonoscopy
Week: 1 2 3 4 5 6 14
E
Yap fl/fl Taz fl/fl
Vil-Cre Yap fl/fl Taz fl/fl
YAP
F
Yap fl/fl Taz fl/fl
Vil-Cre Yap fl/fl Taz fl/fl
AOM 1 month
G
AOM 2 months
Yap fl/fl Taz fl/fl
Vil-Cre Yap fl/fl Taz fl/fl
H
Tumor Volume (mm3)
60
40
20
0
Yap fl/fl Taz fl/fl + AOM
Vil-Cre Yap fl/fl Taz fl/fl + AOM
I
AOM 2 months
Yap fl/fl Taz fl/fl
Vil-Cre Yap fl/fl Taz fl/fl
YAP

Figure S7: YAP is Dispensable for Colon Tumor Growth, Related to Figure 7

(A) Colonoscopy images of mice of the indicated genotypes 8 weeks after injection with Ad-Cre in the colonic mucosa.

(B) Volume of tumors from mice of the indicated genotypes harvested 8 weeks after injection with Ad-Cre in the colonic mucosa. Data are represented as mean ± SEM; n = 4 tumors per genotype.

(C) IHC for YAP in tumors from *Apc*$^{fl/fl}$ *Yap*$^{fl/fl}$ *Taz*$^{fl/fl}$ mice after orthotopic injection with Ad-Cre. Scale bar, 200 μm.

(D) Schematic of sporadic tumor formation in mice of the indicated genotypes, including timeline of azoxymethane (AOM) injection and tissue collection.

(E) IHC for YAP in *Villin-Cre Yap*$^{fl/fl}$ *Taz*$^{fl/fl}$ animals and control littermates. Scale bar, 200 μm.

(F) Colonoscopy images of mice of the indicated genotypes one month after the last AOM injection.

(G) Gross morphology of colons from mice of the indicated genotypes 2 months after the last AOM injection.

(H) Quantification of tumor burden from *Yap*$^{fl/fl}$ *Taz*$^{fl/fl}$ and *Villin-Cre Yap*$^{fl/fl}$ *Taz*$^{fl/fl}$ mice after AOM-induced tumorigenesis. Data are represented as mean ± SEM; n = 4 tumors per genotype.

(I) IHC for YAP in AOM-induced tumors from *Yap*$^{fl/fl}$ *Taz*$^{fl/fl}$ and *Villin-Cre Yap*$^{fl/fl}$ *Taz*$^{fl/fl}$ mice. Scale bar, 100 μm.

Table S4. Primers for RT-qPCR, Related to STAR Methods

Gene	Direction	Sequence 5' to 3'	Source
Human AMOTL2	Forward	AGCTTCAATGAGGGTCTGCTC	Galli et al., 2015
	Reverse	CTGCTGAAGGACCTTGATCACT	
Human CYR61	Forward	CATTCCTCTGTGTCCCCAAGAA	Galli et al., 2015
	Reverse	TACTATCCTCGTCACAGACCCA	
Human GAPDH	Forward	CTGACTTCAACAGCGACACC	This paper
	Reverse	TAGCCAAATTCGTTGTCATACC	
Human LGR5	Forward	CTTCCAACCTCAGCGTCTTC	This paper
	Reverse	TTTCCCGCAAGACGTAACTC	
Mouse AmotL2	Forward	TGGAGACTGTACTGAGGGAGAA	Galli et al., 2015
	Reverse	GAGCCGCTGGATTTCATTTTCC	
Mouse Ankrd1	Forward	CATGATGCTGTGAGGCTGAAC	Galli et al., 2015
	Reverse	CATGATGCTGTGAGGCTGAAC	
Mouse Axin2	Forward	GCCAAGTGTCTCTACCTCATTT	This paper
	Reverse	TCCAGCTCCAGTTTCAGTTTC	
Mouse Cyr61	Forward	AGGTCTGCGCTAAACAACTCA	Galli et al., 2015
	Reverse	ATATTCACAGGGTCTGCCTTCT	
Mouse Gapdh	Forward	AGGTCGGTGTGAACGGATTTG	This paper
	Reverse	TGTAGACCATGTAGTTGAGGTCA	
Mouse Lgr5	Forward	CCTACTCGAAGACTTACCCAGT	This paper
	Reverse	GCATTGGGGTGAATGATAGCA	
Mouse Muc2	Forward	AGGGCTCGGAACTCCAGAAA	This paper
	Reverse	CCAGGGAATCGGTAGACATCG	
Mouse Reg4	Forward	CTGGAATCCCAGGACAAAGAGTG	Sasaki et al., 2016
	Reverse	CTGGAGGCCTCCTCAATGTTTGC	